



## Supplementary Information for

Amygdala lesions eliminate viewing preferences for faces in rhesus monkeys

Jessica Taubert<sup>a1</sup>, Molly Flessert<sup>a</sup>, Susan G. Wardle<sup>b</sup>, Benjamin M. Basile<sup>c</sup>, Aidan P. Murphy<sup>d</sup>, Elisabeth A. Murray<sup>c</sup>, & Leslie G. Ungerleider<sup>a1</sup>

corresponding author Jessica Taubert

Email: [jessica.taubert@nih.gov](mailto:jessica.taubert@nih.gov)

### **This PDF file includes:**

Figs. S1 to S6

Table. S1 to S2

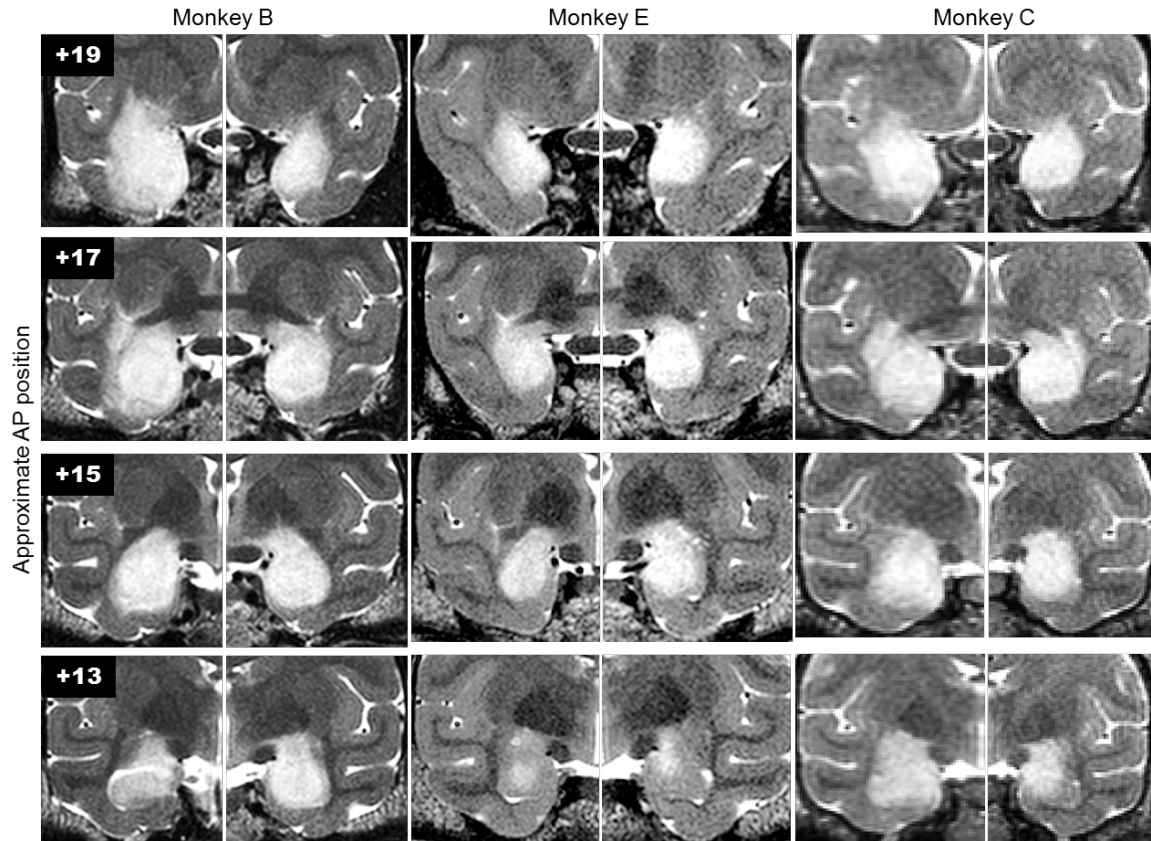


**Fig. S1.** T2 MRI scans of post-surgery hypersignal at different levels. Columns present individual hemispheres, with the left hemisphere on the left, for each monkey. Each row presents coronal images from a different position along the anterior-posterior axis with the most anterior image at the top. Inset numbers are approximate anterior-posterior position with respect to a standard rhesus monkey template. Monkey E also received two additional touch-up injections in the most lateral amygdala tissue in the right hemisphere at approximately AP+16; the resulting scan is not shown here but is included in the quantification of the hypersignal coverage (Table S1).

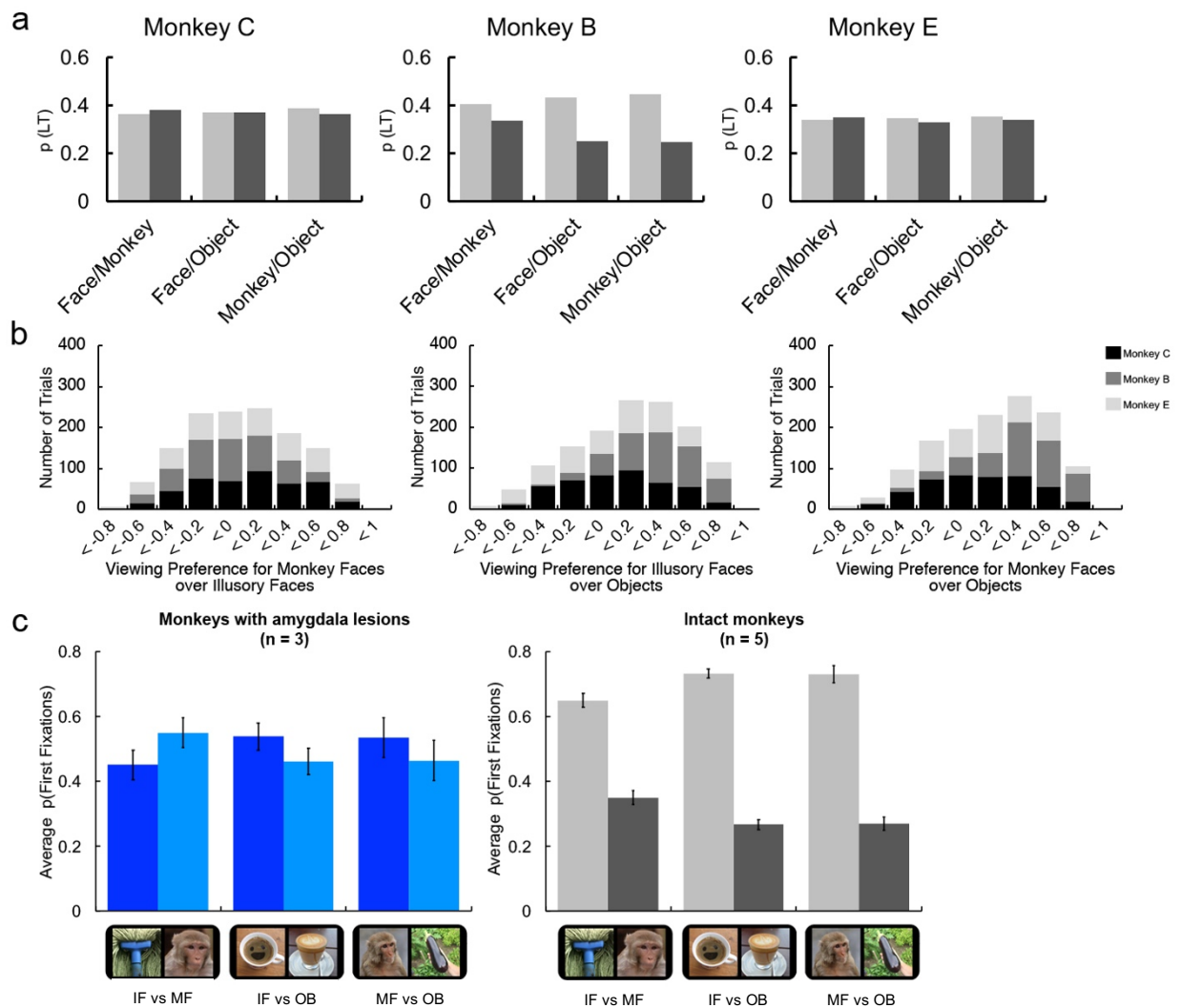


**Fig. S2.** Individual monkey data and first fixations (a) From left to right: bar graphs show proportion looking time towards each stimulus in the three conditions of interest for each monkey individually. Note that Monkey B showed biases in the predicted direction in each of the conditions of interest. The most parsimonious explanation for the partial preservation of the expected preferences in a single subject is the extent or location of the amygdala damage. However, this cannot be verified since the animal is still living. To compare the size of the viewing preferences across the subjects in both groups see Table S2. (b) A stacked histogram where trial indices are broken down by individual subject emphasizes the sizable contribution that Monkey B makes to the distribution's overall skew. (c) Left in blue: A bar graph showing the average proportion of first fixations towards each stimulus type in the three conditions of interest for monkeys with amygdala lesions. Right in grey: Data from historical control monkeys. Reprinted from ref. 1, Copyright (2017), with permission from Elsevier.

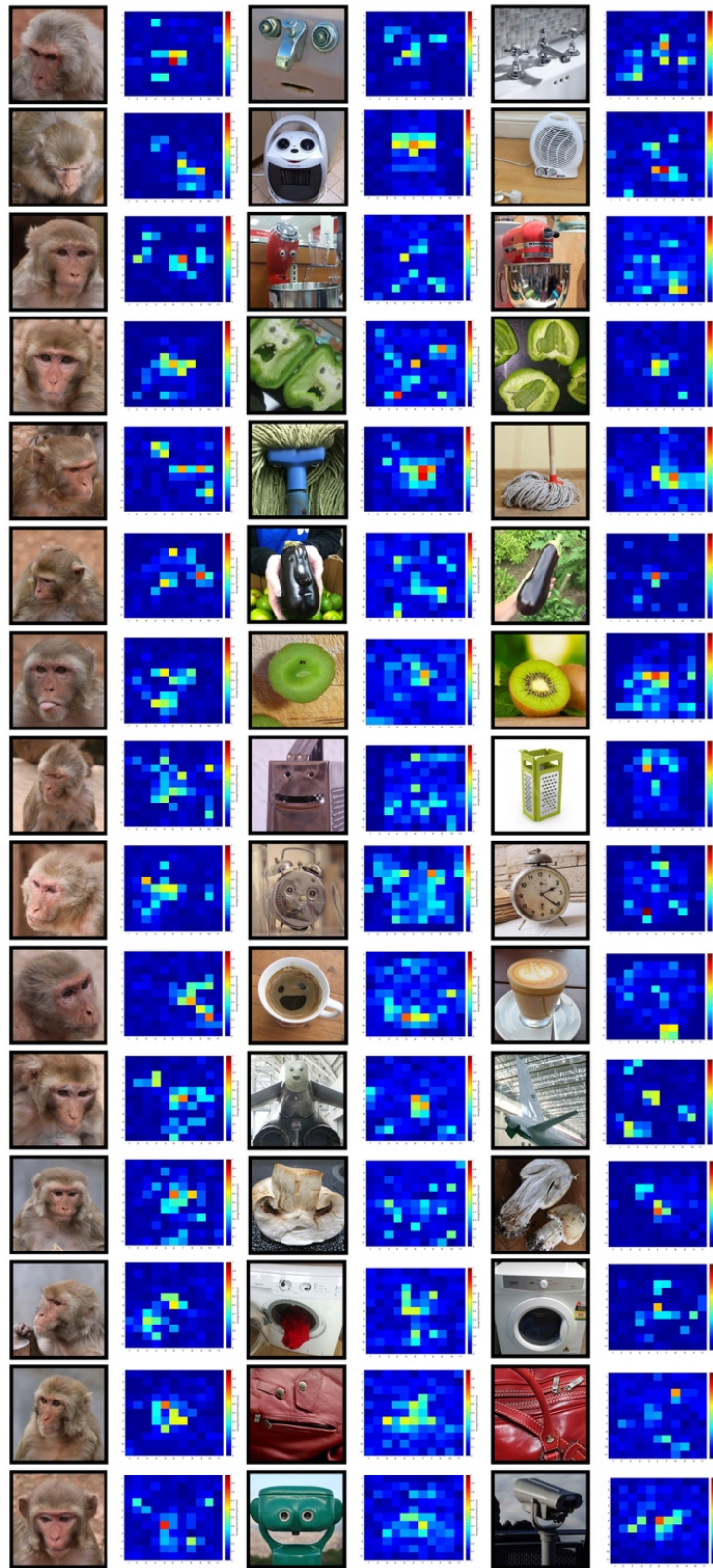


**Fig. S3.** Average fixation density plots for each individual stimulus (unsmoothed). Each fixation density plot is presented on the right of the corresponding stimulus. Data was summed across trials for each subject, normalized to the maximum fixation count, and then averaged across the three amygdalectomized monkeys. The color map is set to 'jet' with hot colors reflecting a greater density of fixations than cool colors.

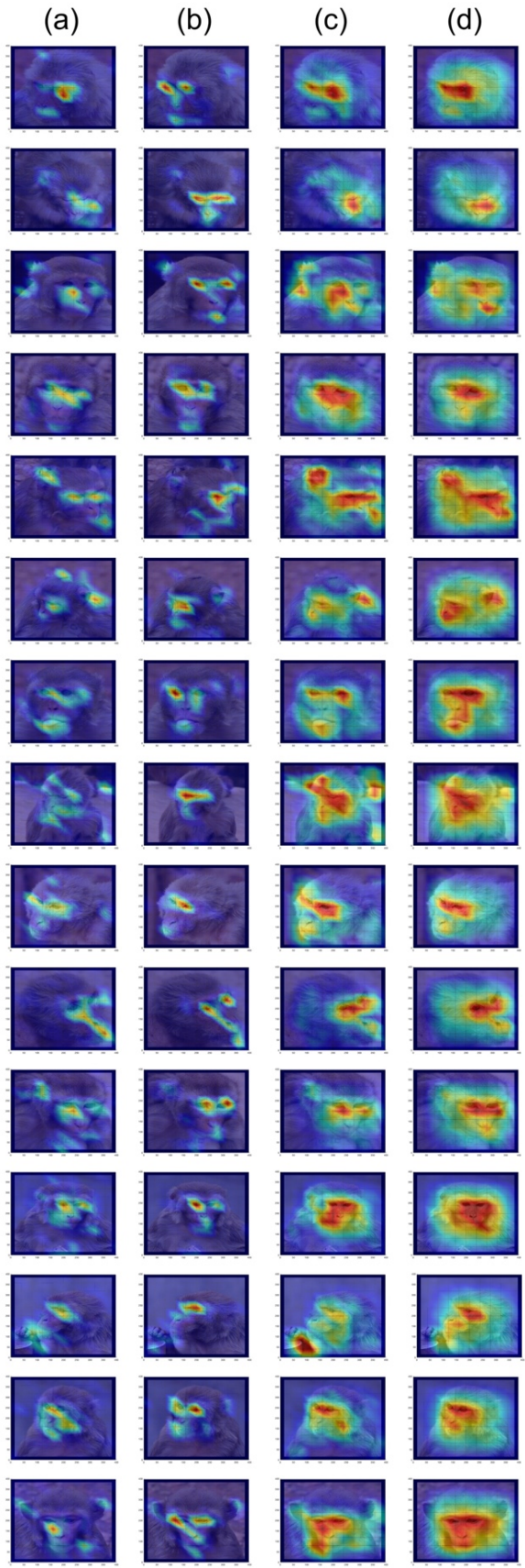


**Fig. S4.** Fixation patterns compared with low-level visual salience for all individual monkey face stimuli. **(a)** The normalized fixation patterns (smoothed) for all 15 face stimuli, averaged across three amygdallectomized subjects, and superimposed on the corresponding stimuli. **(b)** Intact monkey data from the historical controls (normalized, smoothed) for all 15 face stimuli. These maps were used as a proxy for social salience. **(c)** Maps of the visual salience in each stimulus as defined by the Itti-Koch algorithm. The algorithm was run on each stimulus, once, and then normalized to the maximum value (smoothed) **(d)** Maps of the visual salience in each stimulus as defined by the GBVS algorithm (same conventions as (c)). Noting, again, that the algorithm was run on each stimulus only once before normalization.

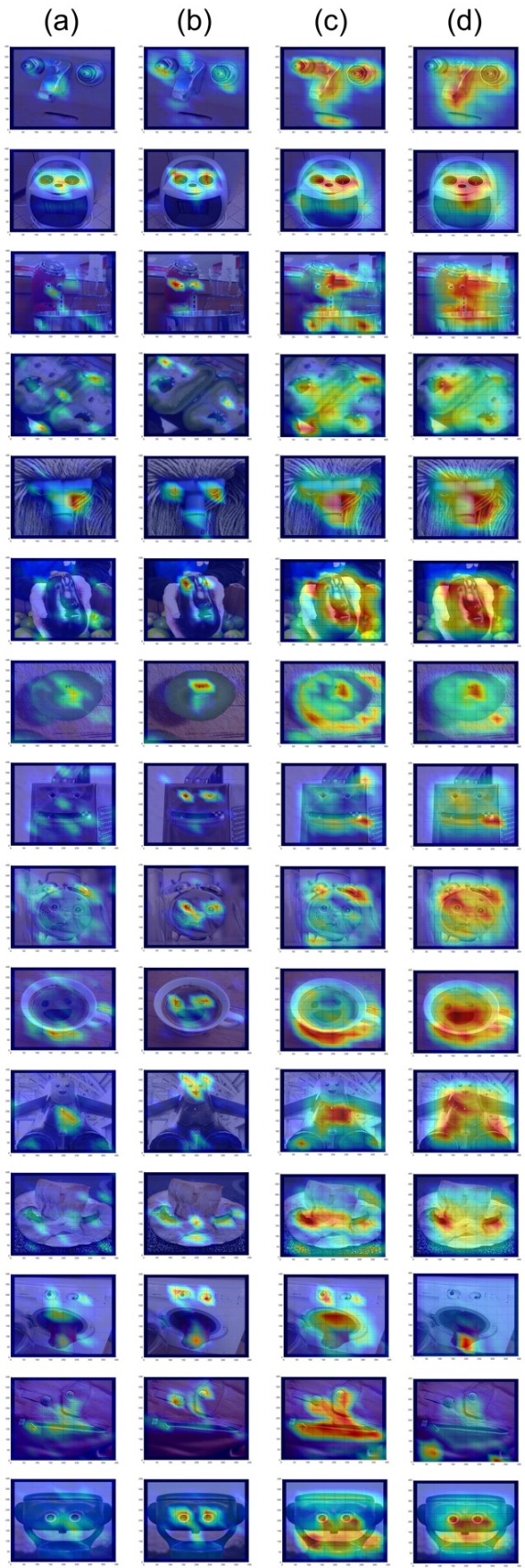




**Fig. S5.** Fixation patterns compared with low-level visual salience for all individual illusory face stimuli. **(a)** Average fixation patterns for monkeys with amygdala lesions ( $n=3$ ), superimposed on the corresponding illusory face stimuli. **(b)** Intact monkey data for the historical controls ( $n = 5$ ) for all 15 illusory face stimuli. **(c)** Maps of visual salience in each illusory face stimulus as defined by the Itti-Koch algorithm. **(d)** Maps of visual salience in each illusory face stimulus as defined by the GBVS algorithm.

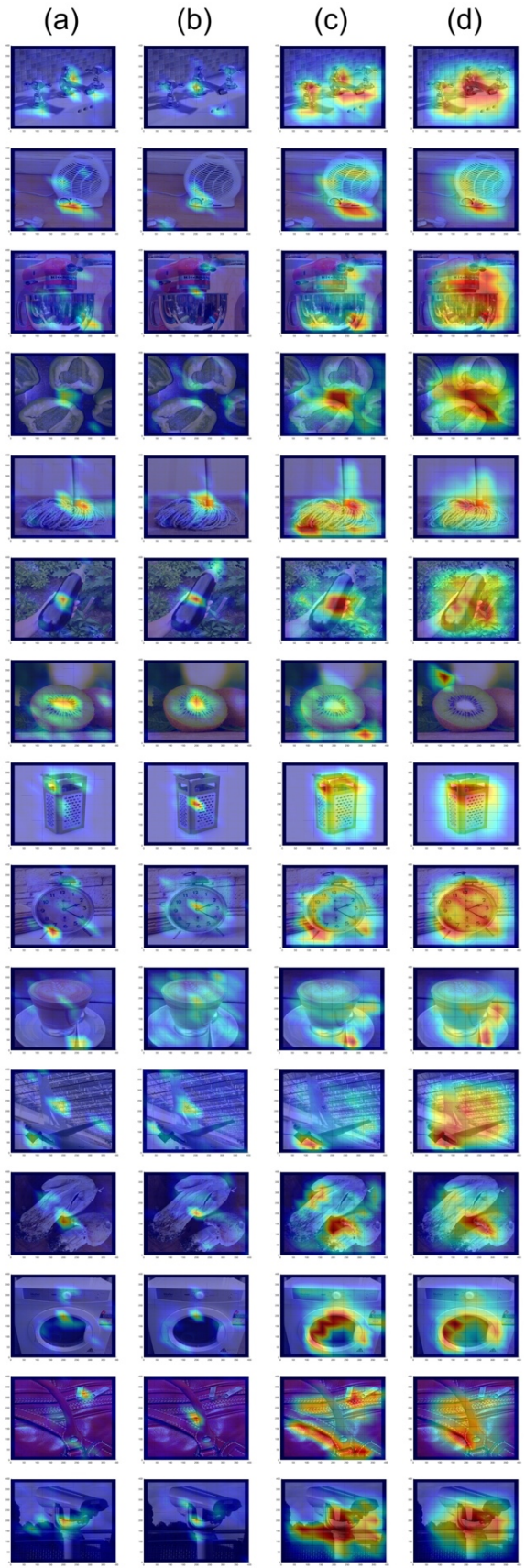


**Fig. S6.** Fixation patterns compared with low-level visual salience for all individual non-face stimuli. **(a)** Average fixation patterns for monkeys with amygdala lesions ( $n=3$ ), superimposed on the corresponding non-face stimuli. **(b)** Intact monkey data from the historical controls ( $n = 5$ ) for all 15 non-face stimuli. **(c)** Maps of visual salience in each illusory face as defined by the Itti-Koch algorithm. **(d)** Maps of visual salience in each illusory face as defined by the GBVS algorithm.

**Table S1. Post-operative T2 MRI signal coverage of the amygdala**

	Left Hemisphere*	Right Hemisphere*	TOTAL*
B	98.5	100	99.3
E	98.1	92.3	95.2
C	100	100	100
Mean	98.9	97.4	98.2

\*Percent of structure covered by hypersignal

**Table S2. Individual monkey data (behavior).**

Group	Subject	Mean difference p(LT)			
		monkey faces - non-face objects	illusory faces - non-face objects	illusory faces - monkey faces	illusory faces - monkey faces
Lesion	B	0.2	0.18		0.07
	E	0.01	0.01		-0.008
	C	0.02	0.001		-0.02
Control	F	0.32	0.31		0.11
	J	0.36	0.35		0.16
	K	0.16	0.23		0.11
	T	0.36	0.34		0.14
	S	0.33	0.43		0.26